Supramolecular Chemistry

International Edition: DOI: 10.1002/anie.201901984
German Edition: DOI: 10.1002/ange.201901984

Nanohoop Rotaxanes from Active Metal Template Syntheses and Their Potential in Sensing Applications

*Jeff M. Van Raden, Brittany M. White, Lev N. Zakharov, and Ramesh Jasti**

Abstract: *The unique optoelectronic properties and smooth, rigid pores of macrocycles with radially oriented π systems render them fascinating candidates for the design of novel mechanically interlocked molecules with new properties. Two high-yielding strategies are used to prepare nanohoop [2]rotaxanes, which owing to the π-rich macrocycle are highly emissive. Then, metal coordination, an intrinsic property afforded by the resulting mechanical bond, can lead to molecular shuttling as well as modulate the observed fluorescence in both organic and aqueous conditions. Inspired by these findings, a self-immolative [2]rotaxane was then designed that self-destructs in the presence of an analyte, eliciting a strong fluorescent turn-on response, serving as proof-of-concept for a new type of molecular sensing material. More broadly, this work highlights the conceptual advantages of combining compact π-rich macrocyclic frameworks with mechanical bonds formed via active-template syntheses.*

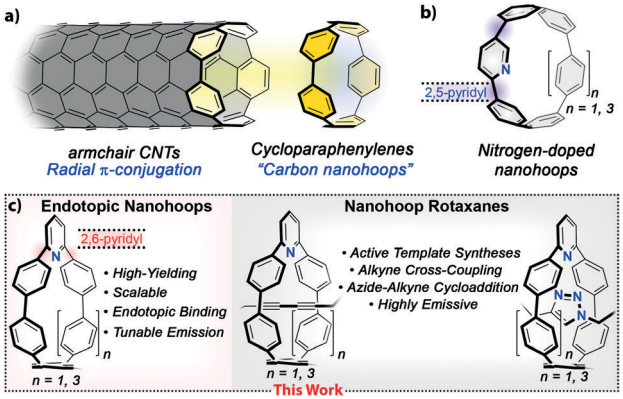

Figure 1. a) Structural relationship between armchair carbon nanotubes and cycloparaphenylenes (carbon nanohoops). b) Previously prepared 2,5-substituted pyridyl-embedded CPPs. c) Nanohoop macrocycles and rotaxanes in this work.

Carbon-rich molecules with closed circuits of delocalized π electrons have been of longstanding interest owing to their unique optical, magnetic, and electronic properties.[1] Of this broad class of molecules, structures that have radially oriented π–π systems pointing inwards to the cavity of a macrocycle have recently emerged as a new class of strained, nonplanar aromatic molecules with unusual properties. Specifically, our laboratory and others have synthesized molecules referred to as carbon nanohoops because of their structural relationship to carbon nanotubes (Figure 1 a).[2] These shape-persistent macrocycles can be prepared with varying size and atomic composition (Figure 1 b),[3] which has unveiled their numerous size-dependent optoelectronic behavior and promising materials applications.[2h,3n] In particular, owing to the tunable and bright fluorescence,[2b] biocompatibility,[3i] and metal binding capabilities,[3c,g,f] we have a growing interest in the development of these π-rich macrocycles for biological applications.

In the field of supramolecular chemistry, mechanically interlocked molecules (MIMs) such as catenanes, rotaxanes, and molecular knots have captured the imagination of chemists, highlighted by the recent Nobel Prize in 2016.[4] A particularly intriguing consequence of threading and/or weaving molecular components is that the resulting structures often possess highly selective molecular recognition sites that would be difficult to access using traditional covalent bonding, a feature that has contributed to a growing interest in employing these architectures as selective sensing platforms,[4d–f] as well as new types of biological materials.[4l,5] In this regard, MIMs comprised of macrocycles with radial π-conjugation could provide new topological landscapes for a variety of applications owing to the exotic optical and electronic properties of structures possessing radial π-conjugation.[3] Only very recently have the first of these fascinating interlocked structures via passive template synthesis approaches have been reported.[6] Alternatively, the active-template method (AT)[4b,c] could be a more powerful approach to these types of MIMs in that it does not rely on formation of a thermodynamically stable preorganized complex and therefore a wider array of structures are possible. Specifically, in the AT approach, a metal bound to the macrocyclic component catalyzes bond formation in the interior of the structure, which gives rise to the interlocked molecules. Herein, we report the syntheses of nanohoop macrocycles that, via an embedded 2,6-pyridyl moiety, participate in AT reactions, ultimately giving rise to a new class of highly compact, fluorescent [2]rotaxanes (Figure 1 c). Moreover, we show that triazole-embedded nanohoop [2]rotaxanes coordinate metals in a reversible manner, which is accompanied by drastic changes in the emission of the macrocyclic fluorophore. Motivated by these findings, we then describe the design and preparation of a self-immolative type of rotaxane sensing platform, ultimately highlighting key

[*] J. M. Van Raden, Dr. B. M. White, Dr. L. N. Zakharov, Prof. Dr. R. Jasti
Department of Chemistry & Biochemistry and Material Science Institute, University of Oregon
Eugene, OR 97403 (USA)
E-mail: rjasti@uoregon.edu
Supporting information and the ORCID identification number(s) for the author(s) of this article can be found under: https://doi.org/10.1002/anie.201901984.

conceptual advantages of forming mechanical bonds with fluorescent carbon nanohoops via AT syntheses.

Inspired by the work of Leigh and Goldup,[4b,g] we initially considered leveraging the coordination ability of our previously reported bipyridyl-embedded nanohoops[3c] in AT reactions to prepare mechanically interlocked nanohoop structures. However, in contrast to macrocycles typically used in AT rotaxane synthesis, a catalytic metal bound to these conformationally rigid nanohoops would direct bond formation to the exterior of the macrocycle.[3c] Thus, our investigations began by first preparing a nanohoop ligand that would direct bond-formation to the interior of the macrocyclic cavity, which we envisioned occurring through the incorporation of a single 2,6-pyridine unit into the nanohoop backbone. Based on the well-established reductive aromatization approach to nanohoop molecules,[3] curved diboronate Suzuki–Miyaura cross-coupling partner **1** (Figure 2) was first

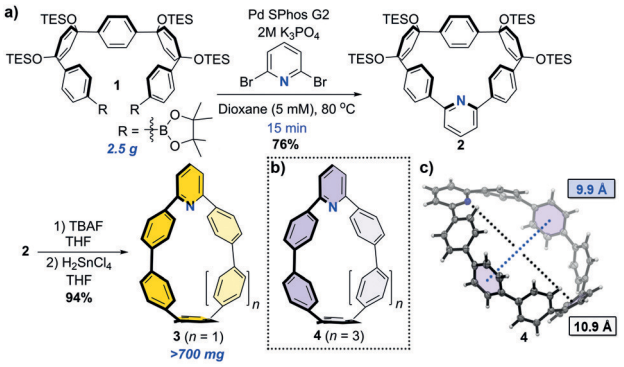

Figure 2. a) Synthetic route used to access ligand **3**. b) Structure of macrocycle **4** and c) observed solid-state structure (ORTEP) of **4**. See the Supporting Information, Figure S1a for synthetic details used to access macrocycle **4**.

prepared.[3j] With boronate **1** in hand, we next explored macrocyclization conditions where under dilute (5 mM) Suzuki–Miyaura cross-coupling conditions with commercially available 2,6-dibromo pyridine, the desired macrocycle **2** was isolated in excellent yield. With macrocycle **2** in hand, a H_2SnCl_4-based aromatization was pursued, which after deprotection with tetrabutylammonium fluoride (TBAF), the target macrocycle **3** was accessed in a 94% yield. Under similar conditions (Supporting Information, Figure S1), larger macrocycle **4** (Figure 2b) was also synthetically accessible, as confirmed by X-ray crystallography (Figure 2c), albeit in slightly reduced yield. Importantly, in stark contrast to our previously reported pyridyl nanohoops, these macrocycles now have a coordination moiety located on the interior of the macrocyclic cavity, as confirmed via X-ray crystallography (Figure 2c). Additionally, as a consequence of breaking molecular orbital symmetry,[3k] it should be noted that both **3** and **4** were fluorescent, with **3** emitting at λ_{max} of 509 nm ($\Phi = 0.14$) and **4** at λ_{max} of 476 nm ($\Phi = 0.62$). Of note, the all *para*-substituted nanohoop with a single embedded pyridine is non-emissive;[3b] a detailed investigation of the result of symmetry breaking on nanohoop fluorescence is disclosed in a separate study.[3o]

We next explored the potential of macrocycles **3** and **4** to participate in AT reactions. As a starting point (Figure 3), we first investigated the well-studied AT Cadiot–Chodkiewicz (AT-CC) reaction.[4h,i] While Glaser couplings have been

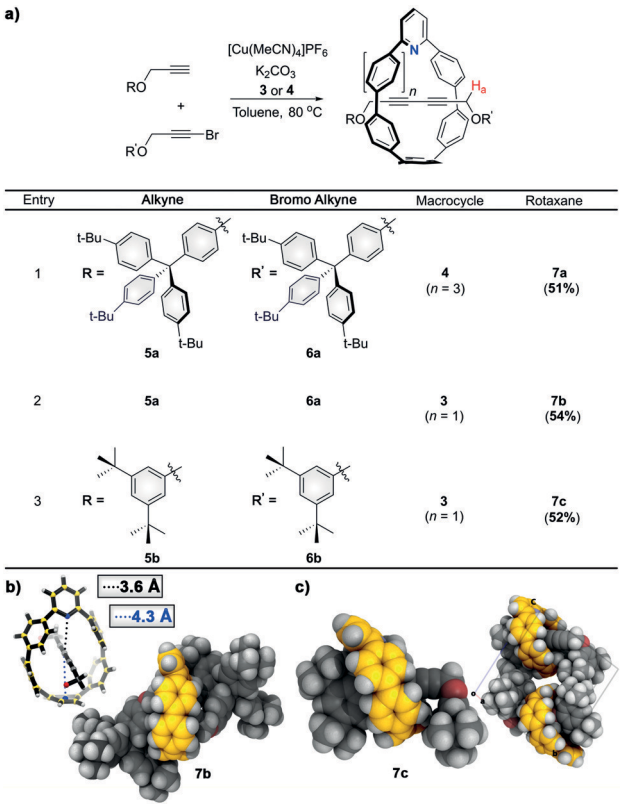

Figure 3. a) Synthesis of nanohoop [2]rotaxanes via AT-CC conditions; solid-state structures (space-filling) of b) [2]rotaxane **7b** and c) **7c**. Macrocycle **3** has been colored yellow while each thread is colored in gray. The inset in (b) shows distances between selected points. For clarity, the trityl groups have been removed.

shown to be quite successful in the preparation of rotaxanes, Cadiot–Chodkiewicz couplings allow for the preparation of unsymmetrical cross-coupled products and often tend to proceed under milder conditions. Based on the observed cavity size of macrocycle **4** in the solid-state (ca. 10 Å, Figure 2c), trityl-stoppered alkyne **5a** and trityl-stoppered bromo-alkyne **6a** were prepared by previously reported procedures.[4j] After optimization, we found that when 1.2 equiv of alkyne **5a** and bromo-alkyne **6a** were subjected to the AT-CC conditions in Figure 3, the desired [2]rotaxane **7a** was isolated in 51% yield. We next tested the ability of smaller macrocycle **3** to participate in an AT-CC reaction, where it was found that the desired rotaxane **7b** formed with no loss in reaction efficiency. While small macrocycles have been explored in some cases,[4g,i] the rigid, shape-persistent nature of macrocycle **3** results in a calculated cavity size of only 7.8 Å (Supporting Information, Figure 5), rendering the formation of **7b** striking. Based on this result, we were curious whether rotaxanes could be prepared using simple, low-molecular-weight stopper groups, which would broaden the types of structures that could be accessed. Accordingly, it was

found that under identical conditions, 3,5-di-*t*-butyl-stoppered rotaxane **7c** was readily formed, whereas unsubstituted benzene rings did not lead to rotaxane formation. Initial structural confirmation of each new [2]rotaxane was acquired by mass spectrometry (Supporting Information, Figures S2 and S3). Furthermore, as is typical with MIMs, multiple upfield NMR shifts were observed in the thread component of each suspected [2]rotaxane, which further suggested a mechanically interlocked structure. For example, proton H_a (see Figure 3a for labels) of the encircled thread in [2]rotaxanes **7a** and **7b** is shifted significantly upfield by nearly 1.5 ppm and 2.0 ppm, respectively, relative to free thread.[4k] Owing to the unusually small nature of macrocycle **3**, we were particularly interested in the structural features of [2]rotaxanes **7b** and **7c**. Indeed, turning to single-crystal X-ray crystallography, the highly congested nature of these π-rich rotaxanes was revealed, where it was found that the cavity of macrocycle **3** is an almost perfect fit for the diyne thread units of both **7b** and **7c** (Figure 3b,c). For example, in the case of **7b**, the observed distance between the central carbon atom of the threaded diyne component and the nitrogen of macrocycle **3** was found to be 3.6 Å (Figure 3b). Additionally, no solvent molecules were observed in either structure, consistent with a tightly packed crystal structure overall. Given that conjugated macrocycles have recently emerged as strong candidates for new types of electronic materials,[3m,l] this result is particularly encouraging, as the ability to thread π-conjugated fragments in close contact could lead to new geometric designs for electron/hole transporting materials.

Owing to the wide range of commercially available azide- and alkyne-functionalized starting materials, we next pursued an active template Cu^I-catalyzed azide–alkyne cycloaddition (AT-CuAAC) reaction.[4b] As a first pass, macrocycle **4** was subjected to conditions (Figure 4) similar to those reported by Leigh et al.,[4b] which provided the corresponding trityl-stoppered rotaxane **9a** in excellent yield. However, when macrocycle **3** was subjected to these conditions using 3,5-dimethyl ester substituted coupling partners (Figure 4, **8c** and **8b**), the desired rotaxane **9b** was formed in 14% yield. After screening various conditions, we found that the addition of acetic acid as well as elevated temperatures (100°C via microwave irradiation) improved the yield considerably, with rotaxane **9b** being isolated in 45% yield (Figure 4, entry 2). While a more detailed investigation of the scope is ongoing, for our work presented herein, we viewed [2]rotaxane **9b** as a particularly versatile intermediate. For example, motivated by our recent report on the biocompatibility of nanohoops[3i] as well the emerging interest in using fluorescent rotaxane architectures in biological environments,[5] **9b** was saponified to access water-soluble [2]rotaxane **9c** (Figure 5a), which

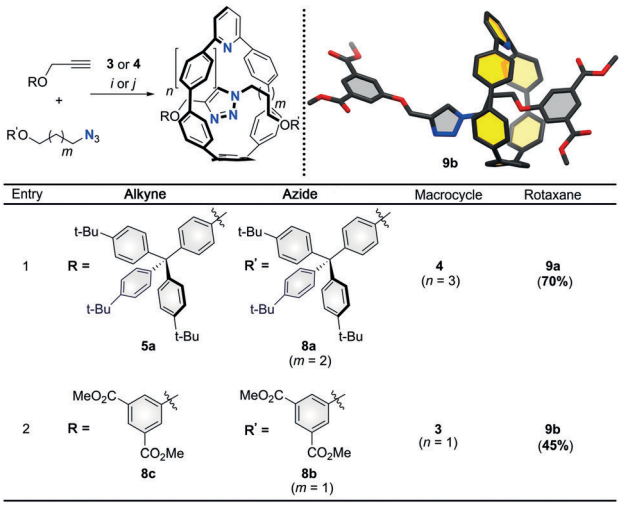

Figure 4. AT-CuAAC conditions used to access triazole rotaxanes **9a** and **9b**. i = $[Cu(MeCN)_4]PF_6$ (0.95 equiv), CH_2Cl_2, rt, 24 h; j = AcOH (20.0 equiv), $[Cu(MeCN)_4]PF_6$ (0.95 equiv), CH_2Cl_2, μW, 100°C, 3 h. X-ray structure of **9b** (top right) showing location of macrocycle **3** (yellow) over triazole thread.

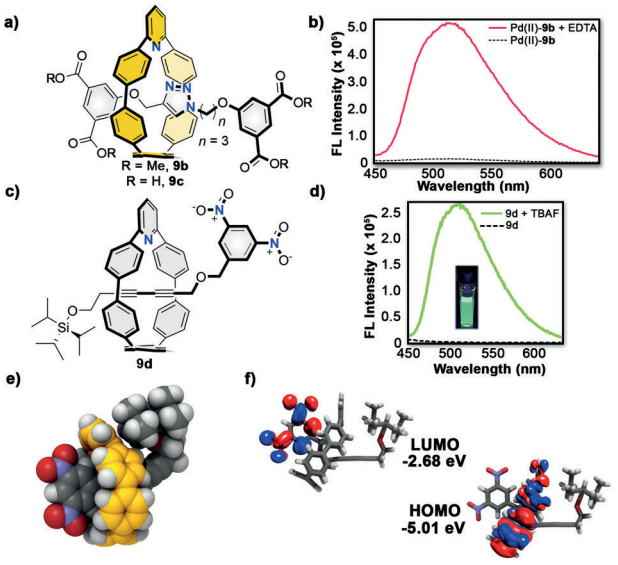

Figure 5. a) Structure of emissive triazole rotaxanes **9b**, **9c** and b) emission spectra: 8.6 μM, $CHCl_3$ (**9b**) of metalated (•••••) and demetalated (——) rotaxane **9b**. c) Structure of non-emissive diyne rotaxane **9d**. d) Emission spectrum (8.6 μM, $CHCl_3$) of **9d** before (•••••) and after (——) addition of 1.0 equivalent of TBAF. e) X-ray structure of [2]rotaxane **9d** in space-filling representation and f) DFT calculated (B3LYP/6–31g) frontier molecular orbitals.

retained the corresponding emission properties ($\Phi = 0.07$) in aqueous conditions. Additionally, apart from biological systems, carboxylate functionalized [2]rotaxanes have also recently been incorporated into metal–organic frameworks,[7] suggesting that this intermediate could act as a new π-rich building block for unusual types of coordination polymers. Ultimately, these results highlight the generality of both the AT-CC and AT-CuAAC reactions, a feature that is expected to provide a variety of new types of π-rich interlocked molecules and materials. Additionally, the narrow cavity of the nanohoops reduce the requirements of the stopper groups that can be employed, furthering the utility of these systems.

Mechanically interlocked molecules bearing nitrogen heteroatoms often engage in a wide range of unique coordination chemistry where, depending on the metal and resulting coordination geometry, features such as molecular

shuttling, switching, and sensing can be enabled.[4] Thus, we were curious if the congested binding pocket of triazole [2]rotaxanes such as **9b** could still participate in metal coordination. To probe this, we next investigated the effects of metalation on **9b** in both the solid state and solution through single-crystal X-ray crystallography, ^{1}H NMR titrations, and fluorescence spectroscopy. In the solid-state (Figure 4), without metal, the macrocycle of **9b** resides over the propyl chain. In solution, a resonance at −1.43 ppm can be observed, indicating that the propyl chain experiences a particularly strong shielding effect, suggesting that the macrocycle resides over the propyl chain. On addition of Cu^I, this signal broadens, but never fully vanishes. Additionally, the appearance of multiple new resonances was observed which indicates the formation of a new species alongside metal-free **9b**. To investigate this further, we then co-crystallized **9b** with 1.0 equiv of $[Cu(MeCN)_4]PF_6$, which revealed that in the solid state, the macrocycle is now localized over the triazole unit with the Cu^I metal coordinated to both the triazole and macrocyclic nitrogen (Supporting Information, Figure S9b). A similar shuttling effect was observed when **9b** was titrated with $[Pd(MeCN)_4](BF_4)_2$. Notably, in presence of Pd^{II}, the observed signals in the ^{1}H NMR spectrum were noticeably sharper relative to that observed with $[Cu(MeCN)_4](PF_6)$, indicating a less dynamic system. Taken together, it can be concluded that, despite the sterically congested environment, triazole embedded rotaxanes bearing macrocycle **3** bind metals such as Cu^I and Pd^{II}, with Pd^{II} acting as a stronger binding metal. From these initial studies, an additional key result was observed; as the amount of Pd^{II} increased, the fluorescence of **9b** decreased. As can be seen in Figure 5b, the addition of 1.0 equiv of $[Pd(MeCN)_4](BF_4)_2$ to **9b** results in a non-emissive rotaxane, that is, Pd^{II}-**9b**. Given that metalation with Pd^{II} effectively traps the fluorophore in a non-emissive state, we expected that demetalation should result in a turn-on response. To validate this, non-emissive Pd^{II}-**9b** was treated with 1.0 equiv of ethylenediaminetetraacetic acid (EDTA), which quickly resulted in a pronounced 30-fold increase in emission (Figure 5b). Encouraged by this result, we were then curious if the emission of water-soluble rotaxane **9c** (Figure 5a) could be modulated in a similar fashion. Indeed, the emission of carboxylate rotaxane **9c** was readily quenched (Supporting Information, Figure S8b) in aqueous media (PBS buffer) by the addition of 1.0 equiv of $[Pd(MeCN)_4](BF_4)_2$ to give Pd^{II}-**9c**. Upon addition of EDTA to this aqueous solution, it was again found (Supporting Information, Figure S8b) that the emission quickly returned, albeit with reduced intensity (10-fold increase).

Inspired by the fluorescence quenching results with metals, we envisioned a perhaps more general sensing platform in which a suitable thread component could serve as both a stopper and fluorescence quencher. Analyte-induced bond cleavage of the thread could then perhaps release the quencher and lead to a turn-on fluorescence response. Encouraged by the ability of electron-deficient C_{60} to quench the emission of [10]CPP,[3l] we hypothesized that macrocycle **3** could temporarily be rendered non-emissive through the incorporation of a cleavable, mechanically bound electron-deficient stopper moiety. To investigate this concept, we prepared a 3,5-dinitro-functionalized rotaxane (**9d**) bearing a fluoride-cleavable triisopropylsilyl (TIPS) stopper group (Figure 5c) via our AT-CC conditions (see the Supporting Information, Figure S1b for details) which we found to be non-emissive (Figure 5d). Importantly, treatment of rotaxane **9d** with 1.0 equiv of tetra-*n*-butylammonium fluoride (TBAF) resulted in a nearly instantaneous dethreading event (Supporting Information, Figure S1c), which was accompanied by a dramatic 123-fold increase in emission intensity (Figure 5d), effectively serving as proof-of-concept for a highly responsive self-immolative rotaxane sensor. Additionally, through density functional theorem (DFT), it was found that the frontier molecular orbitals of **9d** are redistributed relative to macrocycle **3** (Figure 5f). Specifically, for macrocycle **3** (Supporting Information, Figure S5), both the highest-occupied molecular orbital (HOMO) and the lowest-unoccupied molecular orbital (LUMO) reside over the nanohoop backbone. In contrast, in the case of **9d**, the HOMO is localized on the macrocyclic component and the LUMO is localized over the electron-deficient nitrobenzene stopper, consistent with a charge-transfer quenching mechanism. These results highlight the importance of electronic structure in the design of new non-emissive rotaxanes such as **9d**, and we expect that through a computationally guided design approach, a wide range of new analyte-selective, turn-on scaffolds can be prepared. For example, the analyte recognition site (TIPS stopper) of **9d** can likely be replaced by a range of small yet effective analyte-sensitive stopper groups such as boronates, amides, and esters, a key advantage of using a rigid macrocycle with small diameter. Moreover, we anticipate that this design can be applied to our larger macrocycle, **4**, as a means to access different emission wavelength and higher quantum yield. Work is currently underway toward the preparation and application of these structures and will be reported in due course.

In conclusion, this work demonstrates that by embedding a 2,6-pyridine coordination motif into the backbone of a nanohoop macrocycle, a range of diverse [2]rotaxanes are accessible via two different Cu^I-catalyzed active-metal template reactions. Based on fundamental metal coordination experiments with triazole-embedded [2]rotaxanes formed via AT-CuAAC reactions, we have found that two metals, Cu^I and Pd^{II}, effectively shuttle the nanohoop macrocycle along the length of a triazole-functionalized thread. A key result from these studies was the observation that in both organic and aqueous conditions, metal binding is easily monitored by dramatic changes in fluorescence emission. Expanding on this finding, we then designed and prepared, via an AT-CC reaction, a metal-free, non-emissive nanohoop [2]rotaxane that has been stoppered with a fluorescence-quenching 3,5-dinitrobenzyl unit and fluoride-cleavable TIPS group. On bond cleavage, the quenching moiety is no longer in close proximity to the fluorophore, which results in a dramatic 123-fold increase in emission intensity, effectively serving as proof-of-concept for nanohoop rotaxane turn-on fluorescence sensors. Particularly noteworthy is that this self-immolative nanohoop [2]rotaxane was constructed in a modular fashion and therefore should be easily adaptable to other types of analytes and applications. More broadly, we expect that this

active template synthetic strategy will provide efficient pathways for generating a wide array of very compact π-rich interlocked molecules as well as materials. Finally, owing to the highly tunable and rigid π-rich pores, catalytic metals bound to the interior of nanohoops represent an intriguing area of future exploration.

Acknowledgements

Financial support was provided by the National Science Foundation (NSF) (CHE-1808791 and CHE-1800586), the Camille and Henry Dreyfus Foundation, and generous startup funds from the University of Oregon. Mass spectrometry support was provided by NSF (CHE-1625529).

Conflict of interest

The authors declare no conflict of interest.

Keywords: π-conjugation · cycloparaphenylene · mechanical bonds · nanohoops · sensors

How to cite: *Angew. Chem. Int. Ed.* **2019**, *58*, 7341 – 7345
Angew. Chem. **2019**, *131*, 7419 – 7423

[1] a) M. F. L. De Volder, S. H. Tawfick, A. J. Baughman, *Science* **2013**, *339*, 535 – 539; b) M. I. Katsnelson, *Mater. Today* **2007**, *10*, 20 – 27; c) K. S. Novoselov, Z. Jiang, Y. Zhang, S. V. Morozov, H. L. Stormer, U. Zeitler, J. C. Maan, G. S. Boebinger, P. Kim, A. K. Geim, *Science* **2007**, *315*, 1379; d) H. W. Kroto, J. R. Heath, S. C. O'Brien, R. F. Curl, R. E. Smalley, *Nature* **1985**, *318*, 162 – 163; e) Y. Segawa, H. Ito, K. Itami, *Nat. Rev. Mater.* **2016**, *1*, 15002; f) A. Narita, X. Y. Wang, X. Feng, K. Mullen, *Chem. Soc. Rev.* **2015**, *44*, 6616 – 6643.

[2] a) R. Jasti, J. Bhattacharjee, J. B. Neaton, C. R. Bertozzi, *J. Am. Chem. Soc.* **2008**, *130*, 17646 – 17647; b) M. R. Golder, R. Jasti, *Acc. Chem. Res.* **2015**, *48*, 557 – 566; c) E. R. Darzi, R. Jasti, *Chem. Soc. Rev.* **2015**, *44*, 6401 – 6410; d) S. E. Lewis, *Chem. Soc. Rev.* **2015**, *44*, 2221 – 2304; e) M. Majewski, M. Stępień, *Angew. Chem. Int. Ed.* **2019**, *58*, 86 – 116; f) G. Povie, Y. Segawa, T. Nishihara, Y. Miyauchi, K. Itami, *Science* **2017**, *356*, 172 – 175; g) T. Iwamoto, Y. Watanabe, Y. Sakamoto, T. Suzuki, S. Yamago, *J. Am. Chem. Soc.* **2011**, *133*, 8354 – 8361; h) J. B. Lin, E. D. Darzi, R. Jasti, I. Yavuz, K. N. Houk, *J. Am. Chem. Soc.* **2019**, *141*, 952 – 960.

[3] a) E. D. Darzi, E. S. Hirst, C. D. Weber, L. N. Zakharov, M. C. Lonergan, R. Jasti, *ACS Cent. Sci.* **2015**, *1*, 335 – 342; b) J. M. Van Raden, E. D. Darzi, L. N. Zakharov, R. Jasti, *Org. Biomol. Chem.* **2016**, *14*, 5721 – 5727; c) J. M. Van Raden, S. Louie, L. N. Zakharov, R. Jasti, *J. Am. Chem. Soc.* **2017**, *139*, 2936 – 2939; d) S. Hashimoto, E. Kayahara, Y. Mizuhata, N. Tokitoh, K. Takeuchi, F. Ozawa, S. Yamago, *Org. Lett.* **2018**, *20*, 5973 – 5976; e) E. J. Leonhardt, J. M. Van Raden, D. J. Miller, L. N. Zakharov, B. J. Aleman, R. Jasti, *Nano Lett.* **2018**, *18*, 7991 – 7997; f) T. A. Schaub, J. T. Margraf, L. N. Zakharov, K. Reuter, R. Jasti, *Angew. Chem. Int. Ed.* **2018**, *57*, 16348 – 16353; *Angew. Chem.* **2018**, *130*, 16586 – 16591; g) E. Kayahara, V. K. Patel, A. Mercier, E. P. Kundig, S. Yamago, *Angew. Chem. Int. Ed.* **2016**, *55*, 302 – 306; *Angew. Chem.* **2016**, *128*, 310 – 314; h) N. Kubota, Y. Segawa, K. Itami, *J. Am. Chem. Soc.* **2015**, *137*, 1356 – 1361; i) B. M. White, Y. Zhao, T. E. Kawashima, B. P. Branchaud, M. D. Pluth, R. Jasti, *ACS Cent. Sci.* **2018**, *4*, 1173 – 1178; j) V. K. Patel, E. Kayahara, S. Yamago, *Chem. Eur. J.* **2015**, *21*, 5742 – 5749; k) L. Adamska, L. Nayyar, H. Chen, A. K. Swan, N. Oldani, S. Fernandex-Alberti, M. R. Golder, R. Jasti, S. K. Doorn, S. Tretiak, *Nano Lett.* **2014**, *14*, 6539 – 6546; l) T. Iwamoto, Y. Watanabe, T. Sadahiro, T. Haino, S. Yamago, *Angew. Chem. Int. Ed.* **2011**, *50*, 8342 – 8344; *Angew. Chem.* **2011**, *123*, 8492 – 8494; m) M. Ball, Y. Zhong, B. Fowler, B. Zhang, P. Li, G. Etkin, D. W. Paley, J. Decatur, A. K. Dalsania, H. Li, S. Xiao, F. Ng, M. L. Steigerwald, C. Nuckolls, *J. Am. Chem. Soc.* **2016**, *138*, 12861 – 12867; n) E. Kayahara, L. Sun, H. Onishi, K. Suzuki, T. Fukushima, A. Sawada, H. Kaji, S. Yamago, *J. Am. Chem. Soc.* **2017**, *139*, 18480 – 18483; o) T. Lovell, C. Colwell, L. N. Zakharov, R. Jasti, *Chem. Sci.* **2019**, *10*, 3786 – 3790.

[4] a) C. J. Bruns, J. F. Stoddart, *The Nature of the Mechanical Bond: From Molecules to Machines*, Wiley-VCH, Weinheim, **2016**; b) V. Aucagne, K. D. Hanni, D. A. Leigh, P. J. Lusby, D. B. Walker, *J. Am. Chem. Soc.* **2006**, *128*, 2186 – 2187; c) M. Denis, S. M. Goldup, *Nat. Rev. Chem.* **2017**, *1*, 0061; d) M. Denis, Q. Lei, P. Turner, K. A. Jolliffe, S. M. Goldup, *Angew. Chem. Int. Ed.* **2018**, *57*, 5315 – 5319; *Angew. Chem.* **2018**, *130*, 5413 – 5417; e) M. Denis, J. Pancholi, K. Jobe, M. Watkinson, S. M. Goldup, *Angew. Chem. Int. Ed.* **2018**, *57*, 5310 – 5314; *Angew. Chem.* **2018**, *130*, 5408 – 5412; f) J. M. Langton, P. D. Beer, *Acc. Chem. Res.* **2014**, *47*, 1935 – 1949; g) H. Lahlali, K. Jobe, M. Watkinson, S. M. Goldup, *Angew. Chem. Int. Ed.* **2011**, *50*, 4151 – 4155; *Angew. Chem.* **2011**, *123*, 4237 – 4241; h) J. Berná, S. M. Goldup, A.-L. Lee, D. A. Leigh, M. D. Symes, G. Teobaldi, F. Zerbetto, *Angew. Chem. Int. Ed.* **2008**, *47*, 4392 – 4396; *Angew. Chem.* **2008**, *120*, 4464 – 4468; i) L. D. Movsisyan, M. Franz, F. Hampel, A. L. Thompson, R. R. Tykwinski, H. A. Anderson, *J. Am. Chem. Soc.* **2016**, *138*, 1366 – 1376; j) E. A. Neal, S. M. Goldup, *Angew. Chem. Int. Ed.* **2016**, *55*, 12488 – 12493; *Angew. Chem.* **2016**, *128*, 12676 – 12681; k) J. D. Crowley, S. M. Goldup, N. D. Gowans, D. A. Leigh, V. E. Ronaldson, A. M. Slawin, *J. Am. Chem. Soc.* **2010**, *132*, 6243 – 6248; l) J. M. Baumes, J. J. Gassensmith, J. Giblin, J.-J. Lee, A. G. White, W. J. Culligan, W. M. Leevy, M. Kuno, B. D. Smith, *Nat. Chem.* **2010**, *2*, 1025 – 1030; m) Y. Sagara, M. Karman, E. Verde-Sesto, K. Matsuo, Y. Kim, N. Tamaoki, C. J. Weder, *J. Am. Chem. Soc.* **2018**, *140*, 1584 – 1587; n) S. D. P. Fielden, D. A. Leigh, S. L. Woltering, *Angew. Chem. Int. Ed.* **2017**, *56*, 11166 – 11194; *Angew. Chem.* **2017**, *129*, 11318 – 11347.

[5] a) M. W. Ambrogio, C. R. Thomas, Y.-L. Zhao, J. I. Zink, J. F. Stoddart, *Acc. Chem. Res.* **2011**, *44*, 903 – 913; b) R. Barat, T. Legigan, I. Tranoy-Opalinski, B. Renoux, E. Peraudeau, J. Clarhaut, P. Poinot, A. E. Fernandes, V. Aucagne, D. A. Leigh, S. Papot, *Chem. Sci.* **2015**, *6*, 2608 – 2613; c) N. Pairault, R. Barat, I. Tranoy-Opalinski, B. Renoux, M. Thomas, S. C. R. Papot, *Chim.* **2016**, *19*, 103 – 112.

[6] a) Y. Xu, R. Kaur, B. Wang, M. B. Minameyer, S. Gsanger, B. Meyer, T. Drewello, D. M. Guldi, M. von Delius, *J. Am. Chem. Soc.* **2018**, *140*, 13413 – 13420; b) Y.-Y. Fan, D. Chen, Z. Huang, J. Zhu, C. Tung, L. Wu, H. Cong, *Nat. Commun.* **2018**, *9*, 3037; c) P. Bäuerle, M. Ammann, M. Wilde, G. Götz, A. Rang, C. A. Schalley, *Angew. Chem. Int. Ed.* **2007**, *46*, 363 – 368; *Angew. Chem.* **2007**, *119*, 367 – 372.

[7] a) V. N. Vukotic, K. J. Harris, K. Zhu, R. W. Schurko, S. K. Loeb, *Nat. Chem.* **2012**, *4*, 456 – 460; b) V. N. Vukotic, S. K. Loeb, *Chem. Soc. Rev.* **2012**, *41*, 5896 – 5906.

[8] CCDC 1851935, 1851936, 1854176, 1897177, 1897178, and 1897179 contain the supplementary crystallographic data for this paper. These data can be obtained free of charge from The Cambridge Crystallographic Data Centre.

Manuscript received: February 14, 2019
Accepted manuscript online: March 26, 2019
Version of record online: April 17, 2019

